marine drugs

MDPI

Article

Isolation and Structure Elucidation of New Cytotoxic Macrolides Halosmysins B and C from the Fungus *Halosphaeriaceae* sp. Associated with a Marine Alga

Takeshi Yamada [1,*], Kanoko Yoshida [1], Takashi Kikuchi [2] and Tomoya Hirano [1]

[1] Faculty of Pharmacy, Osaka Medical and Pharmaceutical University, 4-20-1, Nasahara, Takatsuki City 569-1094, Osaka, Japan; ompu52116533@s.ompu.ac.jp (K.Y.); tomoya.hirano@ompu.ac.jp (T.H.)
[2] Faculty of Pharmacy, Toho University, 2-2-1, Miyama, Funabashi City 274-8510, Chiba, Japan; takashi.kikuchi@phar.toho-u.ac.jp
* Correspondence: takeshi.yamada@ompu.ac.jp; Tel./Fax: +81-726-90-1085

Abstract: Two new cytotoxic metabolites, halosmysins B and C, have been isolated from the fungus *Halosphaeriaceae* sp. OUPS-135D-4 separated from the marine alga *Sargassum thunbergii*. These chemical structures have been elucidated by 1D and 2D NMR, and HRFABMS spectral analyses. The new compounds had the same 14-membered macrodiolide skeleton as halosmysin A, which was isolated from this fungal strain previously. As the unique structural feature, a diketopiperazine derivative and a sugar are conjugated to the 14-membered ring of halosmysins B and C, respectively. The absolute stereostructures of them were elucidated by the chemical derivatization such as a hydrolysis, the comparison with the known compounds (6*R*,11*R*,12*R*,14*R*)-colletodiol and halosmysin A, and a HPLC analysis of sugar. In addition, their cytotoxicities were assessed using murine P388 leukemia, human HL-60 leukemia, and murine L1210 leukemia cell lines. Halosmysin B was shown to be potent against all of them, with IC_{50} values ranging from 8.2 ± 1.8 to 20.5 ± 3.6 μM, though these values were slightly higher than those of halosmysin A.

Keywords: macrodiolide; halosmysins; *Halosphaeriaceae* sp.; marine alga; cytotoxicity

Citation: Yamada, T.; Yoshida, K.; Kikuchi, T.; Hirano, T. Isolation and Structure Elucidation of New Cytotoxic Macrolides Halosmysins B and C from the Fungus *Halosphaeriaceae* sp. Associated with a Marine Alga. *Mar. Drugs* **2022**, *20*, 226. https://doi.org/10.3390/md20040226

Academic Editor: Eva Zubía

Received: 18 February 2022
Accepted: 22 March 2022
Published: 25 March 2022

1. Introduction

Secondary metabolites produced from marine-derived microorganisms have diverse structures and exhibit unexpected biological activities [1–4]. This study evaluates marine-derived fungi as a seed source for antitumor chemotherapeutic agents. Our group has published papers on the exploratory research of fungal metabolites [5]. Recently, we isolated a cytotoxic compound, halosmysin A (**1**), with a unique skeleton with a thiosilvatin analog conjugated to a 14-membered macrodiolide from the *Halosphaeriaceae* sp. OMPU-135D-4 strain separated from the marine alga *Sargassum thunbergii*. (Figure 1) [6]. The related polyketide macrodiolides such as colletodiol (**4**), colletoketol (grahamimysins A), colletoll, and colletallol from *Colletotrichum capsici* [7]; grahamimysins A_1 and B from *Cytospora* sp. [8–10]; 9,10-dihydrocolletodiol from *Varicosporina ramulosa* [11]; clonostachydiol from *Clonostachys cylindrospora* [12], *Gliocladium* sp. [13], and *Xylaria* sp. [14,15]; 4-keto-clonostachydiol from *Gliocladium* sp. [13,16]; cordybislactone from *Cordyceps* sp. [14]; acremonol and acremodiol from anunidentified *Acremonium*–like anamorphic fungus [17]; and acaulones from *Acaulium* sp. [18] exhibited diverse activities such as antimicrobial, antiosteoporosis, tyrosine kinase inhibition, anthelmintic, and cytotoxicity. The stereochemistry of these macrodiolides, consisting of two unsymmetrical subunits, was grouped into two types: the colletodiol-type, possessing 6*R*,14*R* and the clonostachydiol-type, possessing 6*S*,14*S* (Figure S1). In a previous study, the absolute configuration of **1** was established to be 6*R*,14*R* upon a comparison with known compound **4** [6]. In the present study, an ongoing search for cytotoxic metabolites from this strain led to the isolation of two new

14-membered macrodiolides designated as halosmysins B (**2**) and C (**3**) (Figure 1). The structural analysis of **2** by ^{1}H and ^{13}C nuclear magnetic resonance (NMR) spectroscopic techniques showed that **2** has the same planar structure as **1**. On the other hand, the alkaline hydrolysis of **3** gave the enantiomer of 5-hydroxy-(2*E*)-hexenoic acid derived from **1** and **4**. This paper reports the absolute stereostructures of **2** and **3**, including nuclear Overhauser effect spectroscopy (NOESY) data, information garnered from the *J* values in the ^{1}H NMR spectrum, and a plausible biosynthetic proposal. The cytotoxic activities of these compounds against the murine P388 leukemia, human HL-60 leukemia, and murine L1210 leukemia cell lines are also described.

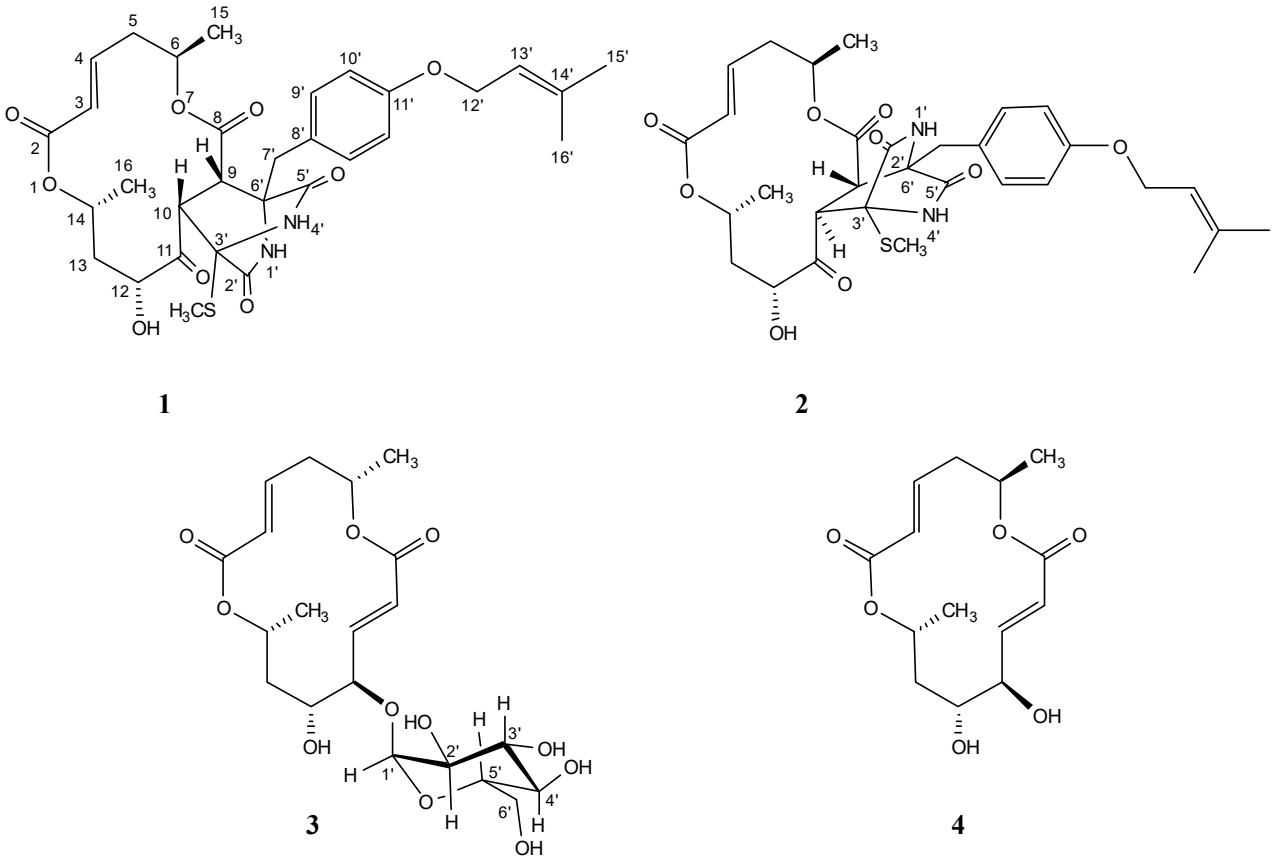

Figure 1. Halosmysins A–C (**1**–**3**) and colletodiol (**4**) isolated from *Halosphaeriaceae* sp. strain.

2. Results and Discussion

Halosphaeriaceae sp., a fungal strain from *S. thunbergii*, was incubated at 27 °C for six weeks in a medium (70 L) containing 1% glucose, 1% malt extract, and 0.05% peptone in artificial seawater adjusted to pH 7.5. The EtOAc extract of the culture filtrate after incubation was purified on a silica gel column, followed by reverse-phase high-performance liquid chromatography (HPLC), affording halosmysins B (**2**) (0.8 mg) and C (**3**) (5.5 mg). The structural determination of halosmysin A (**1**) has been reported [6], and (6*R*,11*R*,12*R*,14*R*)-colletodiol (**4**) was identified by comparison with the data reported by MacMillan et al. [7].

Halosmysin B (**2**) had the formula $C_{31}H_{38}N_2O_9S$ established by *m*/*z* 615.2378 $[M + H]^+$ (calcd for $C_{31}H_{39}N_2O_9S$: 615.2376) by high-resolution fast atom bombardment mass spectrometry (HRFABMS) (Figure S8). The Fourier transform infrared spectrum revealed peaks at 3378 and 1712 cm^{-1}, which were assigned to the stretching vibrations of hydroxy and carbonyl groups, respectively (Figure S9). An inspection of the ^{1}H and ^{13}C NMR spectra (Table 1 and Table S1, Figures S2–S7) of **2** using distortionless enhancement by polarization transfer (DEPT) and ^{1}H-^{13}C correlation spectroscopy (HSQC) showed the presence of the following: one thiomethyl group (3′-SCH_3); two secondary methyls (C-15 and C-16); two olefinic methyls (C-15′ and C-16′);

four sp^3-hybridized methylenes (C-5, C-13, C-7′, and C-12′); one of which is an oxygen-bearing sp^3-methylene (C-12′); five sp^3-methines (C-6, C-9, C-10, C-12, and C-14); three of which are oxygen-bearing sp^3-methines (C-6, C-12, and C-14); seven sp^2-methines (C-3, C-4, C-9′, C-10′, and C-13′); two quaternary sp^3-carbons (C-3′, and C-6′); three quaternary sp^2-carbons (C-8′, C-11′ and C-14′); and five carbonyl groups (C-2, C-8, C-11, C-2′, and C-5′). The correlations observed in ^{1}H-^{1}H correlation spectroscopy (COSY) and the ^{1}H-^{13}C heteronuclear multiple bond correlation (HMBC) spectra showed that **2** had the same planar structure as **1**, which was a 14-membered macrodiolide conjugated to a thiosilvatin analog, that is, a 3,6-bis(methylthio)-2,5-piperazinedione derivative (Table S1). The HMBC correlations from H-1′ (NH) to C-3′and C-7′, from H-4′ (NH) to C-6′, from S-CH_3 to C-3′, from H-7′ to C-5′, C-6′, C-8′, and C-9′, from H-9 to C-6′, from H-10 to C-3′, and H-7′ to C-9 suggested that the 14-membered bislactone moiety and the diketopiperazine derivative were bound between C-9 and C-6′ and between C-10 and C-3′ (Table S1). The NMR chemical shifts of these signals closely resembled those of **1** except for the NMR signals for the thiosilvatin moiety [proton signals—H-9 (δ_H 3.59 d), H-10 (δ_H 4.81 d), H-7′ (δ_H 2.99 d, 3.56 d), and H-10′ (δ_H 7.30 d); carbon signals—C-9 (δ_C 52.6), C-10 (δ_C 52.4), C-5′ (δ_C 169.5), and C-6′ (δ_C 62.2)]. This suggested that **2** was a stereoisomer of **1** around the thiosilvatin moiety.

The relative configuration and the conformation of **2** were investigated by NOESY experiments (Table S1 and Figure 2 and Figure S5). For the 14-membered ring moiety of **2**, the NOESY correlations between H-3 and H-5β and between H-4 and H-6, and the large coupling constants ($J_{5\beta,6}$ = 12.6 Hz and $J_{5\beta,4}$ = 10.8 Hz) showed that the angle between bond C-6–C-5 and bond C-4–C-3 was as that of **1**. Furthermore, the NOESY correlations from H-16 to H-13α and H-13β and the large coupling constants ($J_{13\beta,14}$ = 11.4 Hz) revealed the angle between bond C-14–C-16 and bond C-13–C-12 (Figure 2 and Tables S1 and S2). The NOESY correlations between H-9 and H-4′ (NH) and between H-10 and H-4′ (NH) were observed in **1**. However, the correlation observed in **2** was only between H-10 and H-4′ (NH), and H-9 correlated with H-1′ (NH). The NOESY correlations (H-9/H-3, H-10/H-12, and H-10/3′-SCH_3) suggested that the orientation for H-10 was opposite to that of H-9. The above evidence showed that the stereo-arrangements of H-3′ and H-6′ in the diketopiperazine ring of **2** were opposite to those of **1**. Thus, the relative configuration of **2** was established, as shown in Figure 2, which was a stereoisomer of **1** at C-10, C-3′, and C-6′. As described elsewhere [6], the absolute configuration of **1** was determined by alkaline hydrolysis, i.e., the ^{1}H NMR spectrum and the specific rotation of the reaction product, 5-hydroxy-(2*E*)-hexenoic acid, were identified with those of the hydrolyzed product from (6*R*,11*R*,12*R*,14*R*)-colletodiol (**4**). The reaction gave (–)-5-hydroxy-(2*E*)-hexenoic acid when the same procedure was applied to **2**, as expected. Hence, the absolute stereostructure of **2** was 6*R*,9*S*,10*R*,12*R*,14*R*,3′*S*,6′*R* (Figure 2).

In a previous study, we hypothesized the biosynthetic pathway of **1** from colletoketol, which was derived from **4** via the oxidative process [6]. The 3*R*-derivative shown in Scheme 1, which could be formed by the elimination of the SCH_3 group in a 3*R*,6*R*-bis(methylthio)-2,5-piperazinedione derivative, such as *cis*-bis(methylthio) silvatin [19], could be attacked by the π-electron at C-9 in colletoketol, forming a bond between C-9 and C-6′ in **1**. The C-10 in the macrodiolide could be attacked from below by C-3 in 3*R*-piperazinedione, forming a bond between C-10 and C-3′ in **1** (Scheme 1). On the other hand, **2** could be formed by the attack of C-3 in the 3*S*-derivative formed from a 3*S*,6*S* or 3*S*,6*R*-bis(methylthio)-2,5-piperazinedione derivative, such as Sch 54,794 [20,21] or *trans*-bis(methylthio)silvatin [20], to above of C-10 in colletoketol. This final nucleophilic attack was on the opposite side of that forming **1**.

Table 1. NMR spectral data for **1** [b], **2** [b], and **3** [c].

	1				**2**				**3**			
Position	δ_H [a]		δ_C		δ_H [a]		δ_C		δ_H [a]		δ_C	
2			165.6	(s)			166.2	(s)			166.9	(s)
3	5.64	d (16.2)	125.3	(d)	5.66	d (16.4)	124.6	(d)	5.78	d (16.2)	126.8	(d)
4	6.78	ddd (16.2,10.2,6.0)	143.5	(d)	6.83	ddd (16.4,10.8,6.0)	145.2	(d)	6.68	ddd (16.2,12.0,4.2)	146.0	(d)
5α	2.48	ddd (13.2,6.0,1.2)	39.0	(t)	2.53	ddd (13.2,6.0,1.8)	40.0	(t)	2.27	ddd (13.2, 12.0, 12.0)	42.0	(t)
5β	2.23	ddd (13.2,13.2, 10.2)			2.25	ddd (13.2,12.6,10.8)			2.58	ddd (13.2,4.2,4.2)		
6	5.30	dqd (13.2,6.0,1.2)	69.9	(d)	5.31	dqd (12.6,6.6,1.8)	69.9	(d)	5.29	dqd (12.0,6.0,4.2)	70.1	(d)
8			168.9	(s)			169.0	(s)			167.8	(s)
9	3.38	d (3.0)	51.9	(d)	3.59	d (3.6)	52.6	(d)	6.08	dd (15.6,0.6)	125.2	(d)
10	4.57	d (3.0)	51.0	(d)	4.81	d (3.6)	52.4	(d)	6.77	dd (15.6,6.0)	147.2	(d)
11			208.2	(s)			208.0	(s)	3.96	ddd (9.0,6.0,0.6)	83.8	(d)
12	4.55	d (7.8)	75.6	(d)	4.56	dd (9.0,8.4)	75.1	(d)	3.76	ddd (9.0,6.6,1.2)	72.6	(d)
13α	1.96	ddd (14.4,7.8,3.0)	37.4	(t)	1.93	ddd (15.0,8.4,2.4)	37.3	(t)	1.92	dd (16.2,4.2)	37.1	(t)
13β	2.64	ddd (14.4,12.0, 1.2)			2.60	ddd (15.0,11.4,1.2)			1.48	ddd (16.2,6.6,2.4)		
14	5.23	dqd (12.0,6.0,3.0)	65.5	(d)	5.25	dqd (11.4,6.6,2.4)	65.8	(d)	5.13	qdd (6.6,4.2,2.4)	69.7	(d)
15	1.44	d (6.0)	20.9	(q)	1.40	d (6.6)	20.5	(q)	1.36	d (6.0)	20.6	(q)
16	1.26	d (6.0)	20.2	(q)	1.27	d (6.6)	20.3	(q)	1.33	d (6.6)	18.4	(q)

Table 1. *Cont.*

	1				**2**				**3**			
Position	δ_H [a]		δ_C		δ_H [a]		δ_C		δ_H [a]		δ_C	
12-OH	Not observed				3.31	3.31			Not observed		Not observed	
1′	5.73	s			5.84	s			5.00	d (3.6)	102.9	(d)
2′			165.7	(s)			165.4	(s)	3.43	dd (9.6,3.6)	73.9	(d)
3′			68.6	(s)			68.6	(s)	3.67	dd (9.6,9.6)	75.1	(d)
4′	5.95	s			6.26	s			3.34	dd (10.2,9.6)	71.4	(d)
5′			170.9	(s)			169.5	(s)	3.55	dt (10.2,3.6)	74.3	(d)
6′			63.7	(s)			62.2	(s)	3.64	d (3.6)	62.1	(t)
7′A	2.83	d (14.4)	33.0	(t)	2.99	d (14.4)	34.2	(t)				
7′B	3.88	d (14.4)			3.56	d (14.4)						
8′			125.5	(s)			125.0	(s)				
9′	6.83	d (9.0)	131.7	(d)	6.90	d (8.4)	131.6	(d)				
10′	7.10	d (9.0)	115.2	(d)	7.30	d (8.4)	115.6	(d)				
11′			158.5	(s)			158.7	(s)				
12′	4.47	d (7.2)	64.8	(t)	4.51	d (6.0)	64.8	(t)				
13′	5.47	br t (7.2)	119.5	(d)	5.50	br t (6.0)	119.5	(d)				
14′			138.4	(s)			138.5	(s)				
15′	1.79	s	25.8	(q)	1.81	s	25.8	(q)				
16′	1.74	s	18.2	(q)	1.76	s	18.2	(q)				
S-CH_3	2.25	s	13.0	(q)	2.34	s	12.4	(q)				

[a] ^{1}H chemical shift values (δ ppm from $SiMe_4$) followed by multiplicity and then the coupling constants (J/Hz). [b] 600 MHz (^{1}H NMR), 150 MHz (^{13}C NMR) in $CDCl_3$. [c] 600 MHz (^{1}H NMR), 150 MHz (^{13}C NMR) in MeOH-d_4.

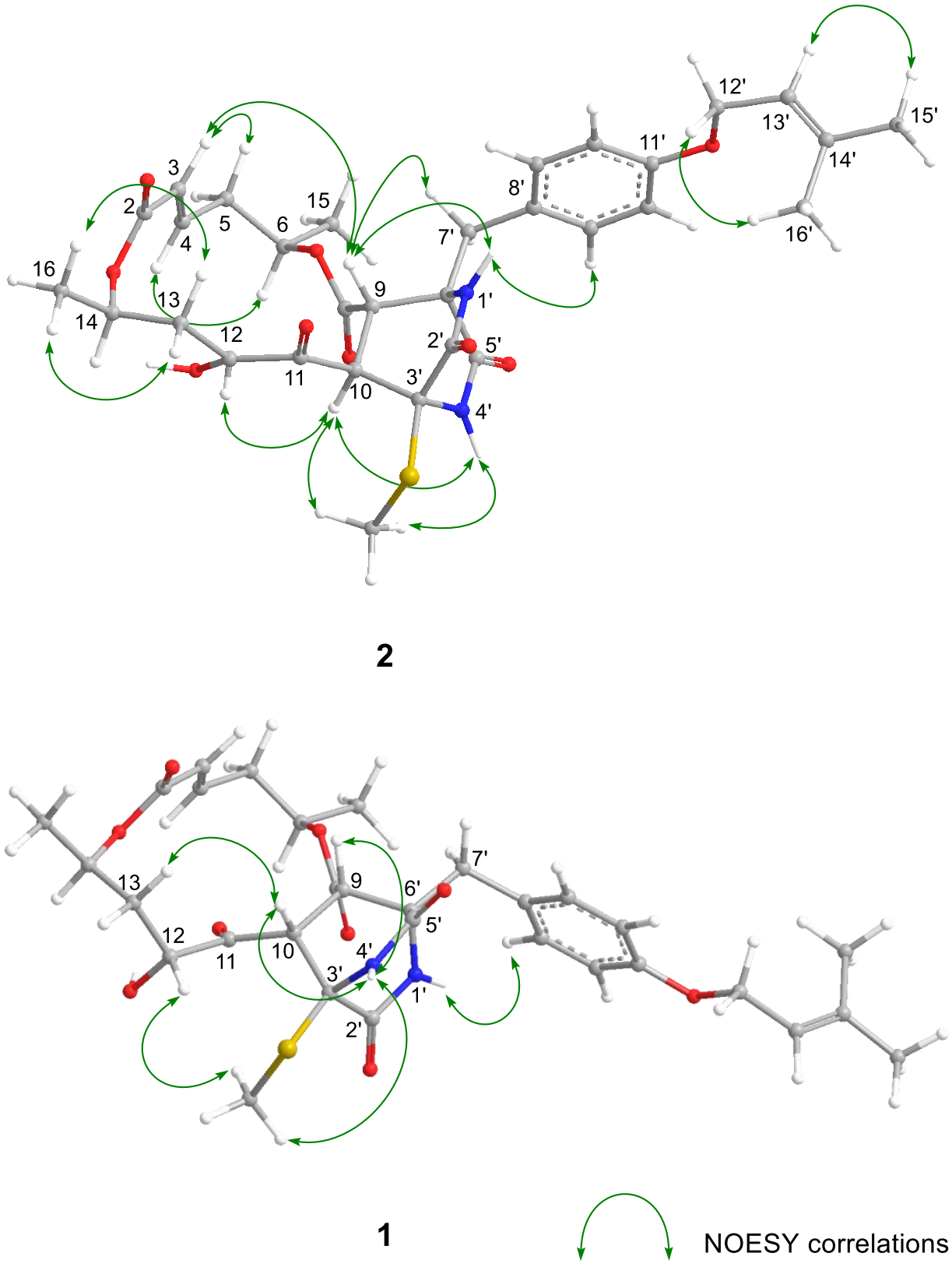

Figure 2. Key NOESY correlations for **1** and **2**.

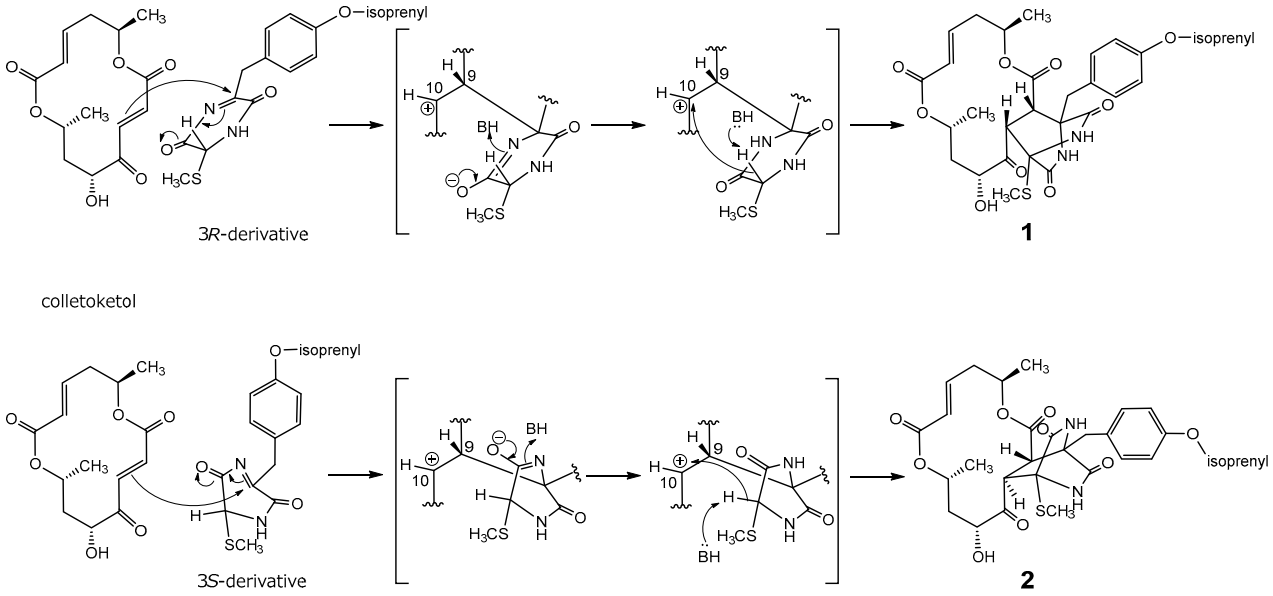

Scheme 1. Plausible biosynthetic pathway toward **1** and **2**.

Halosmysin C (**3**) was assigned the molecular formula $C_{20}H_{30}O_{11}$ from HRFABMS (Figure S16). The ^{1}H and ^{13}C NMR spectra of **3** (Table 1 and Table S2, and Figures S10–S15) showed the signals for the 14-membered macrodiolide skeleton, which were similar to those of **1** and **2**, except for that the signals for the double bond [proton signals; H-9 (δ_H 6.08 dd) and H-10 (δ_H 6.77 dd), carbon signals; C-9 (δ_C 125.2) and C-10 (δ_C 147.2)] were observed. Therefore, **3** was derived from colletodiol (**4**). For the partial molecule conjugated to the macrodiolide skeleton, the signals for the bis(methylthio)silvatin derivative observed in **1** and **2** disappeared. However, those for a sugar [the proton signals—H-1′ (δ_H 5.00 d), H-2′ (δ_H 3.43 dd), H-3′ (δ_H 3.67 dd), H-4′ (δ_H 3.34 d), H-5′ (δ_H 3.55 dt), and H-6′ (δ_H 3.64 d); the carbon signals—C-1′ (δ_C 102.9), C-2′ (δ_C 73.9), C-3′ (δ_C 75.1), C-4′ (δ_C 71.4), C-5′ (δ_C 74.3), and C-6′ (δ_C 62.1)] appeared. The HMBC correlation from H-11 to the anomeric carbon C-1′ showed the sugar was conjugated to C-11 in **3**. The correlations (H-2′/H-4′ and H-3′/H-5′) in the NOESY experiment and the coupling constant ($J_{1',2'}$ 3.6, $J_{2',3'}$ 9.6, $J_{3',4'}$ 9.6, and $J_{4',5'}$ 10.2 Hz) in the ^{1}H NMR spectrum in **3** showed that the sugar in this molecular structure was α-glucose (Figure 3 and Table S2).

Alkaline hydrolysis, which was the same procedure used with **1** and **2**, was carried out to determine the absolute configuration of **3**. The purification of the reaction mixture gave two carboxylic acids. The ^{1}H NMR spectral data of them were in perfect agreement with those of the carboxylic acids obtained by the hydrolysis of **4**, 5-hydroxy-(2*E*)-hexenoic acid and 4,5,7-trihydroxy-(2*E*)-octenoic acid, respectively (Scheme 2). Furthermore, the specific rotations of 4,5,7-trihydroxy octenoic acid obtained from **3** and **4** were in agreement. However, the specific rotations of **3**-derived 5-hydroxy hexenoic acid showed a positive sign ($[\alpha]_D$ + 9.1), and that of **4**-derived showed a negative sign ($[\alpha]_D$ − 14.3). The evidence showed that the absolute configuration in the 14-membered macrodiolide moiety of **3** is 6*S*,11*R*,12*R*,14*R*. The absolute stereostructure of the sugar conjugated to C-11 in the 14-membered ring was determined by the discrimination between the aldose enantiomers using reversed-phase HPLC. In producing the standard samples, D- and L-glucose were treated with L-cysteine methyl ester hydrochloride and *o*-torylisothiocyanate in pyridine, respectively. Each reaction mixture was analyzed by HPLC, which showed retention times for the D-glucose and L-glucose derivatives of 17.7 min and 12 min, respectively [22]. After the hydrolysis by hydrochloric acid of **3**, the same procedure as standard gave the HPLC peak at 17.7 min. In addition, the ^{1}H NMR spectral data of the sugar derivative from **3** were in good agreement with those of the D-glucose derivative. Therefore, **3** was confirmed to be the glycoside with α-D-glucose.

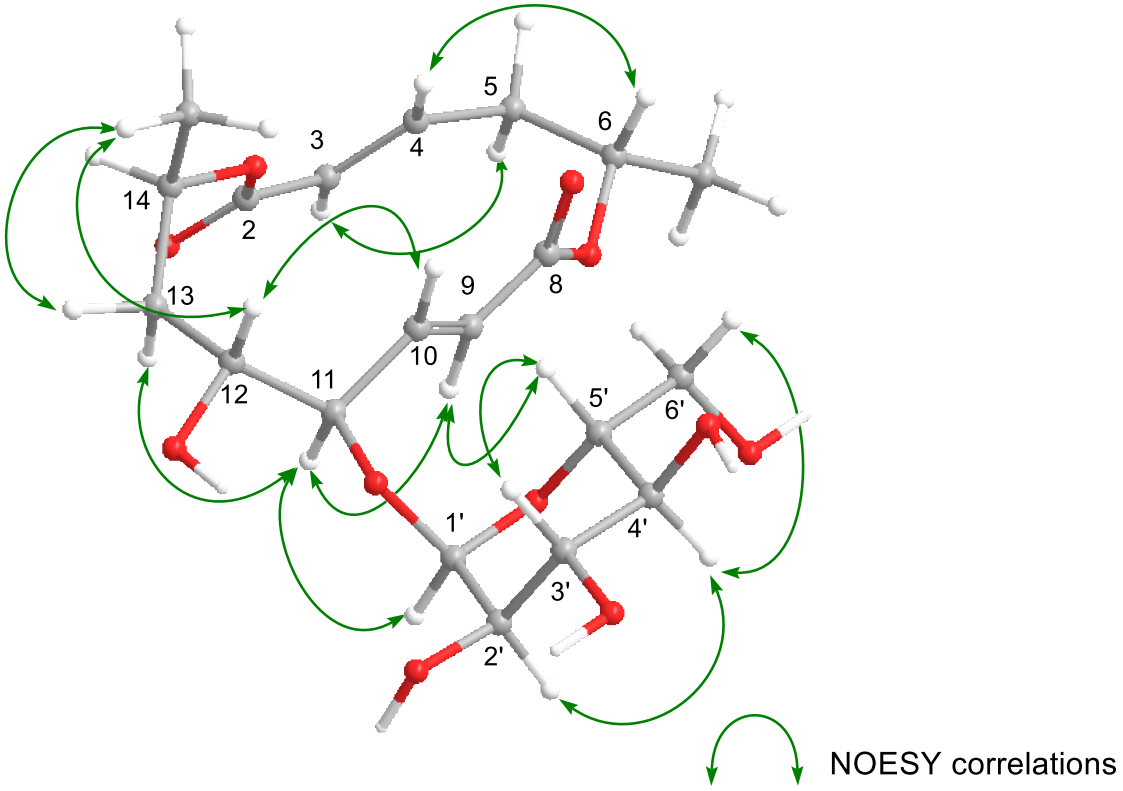

Figure 3. Key NOESY correlations for **3**.

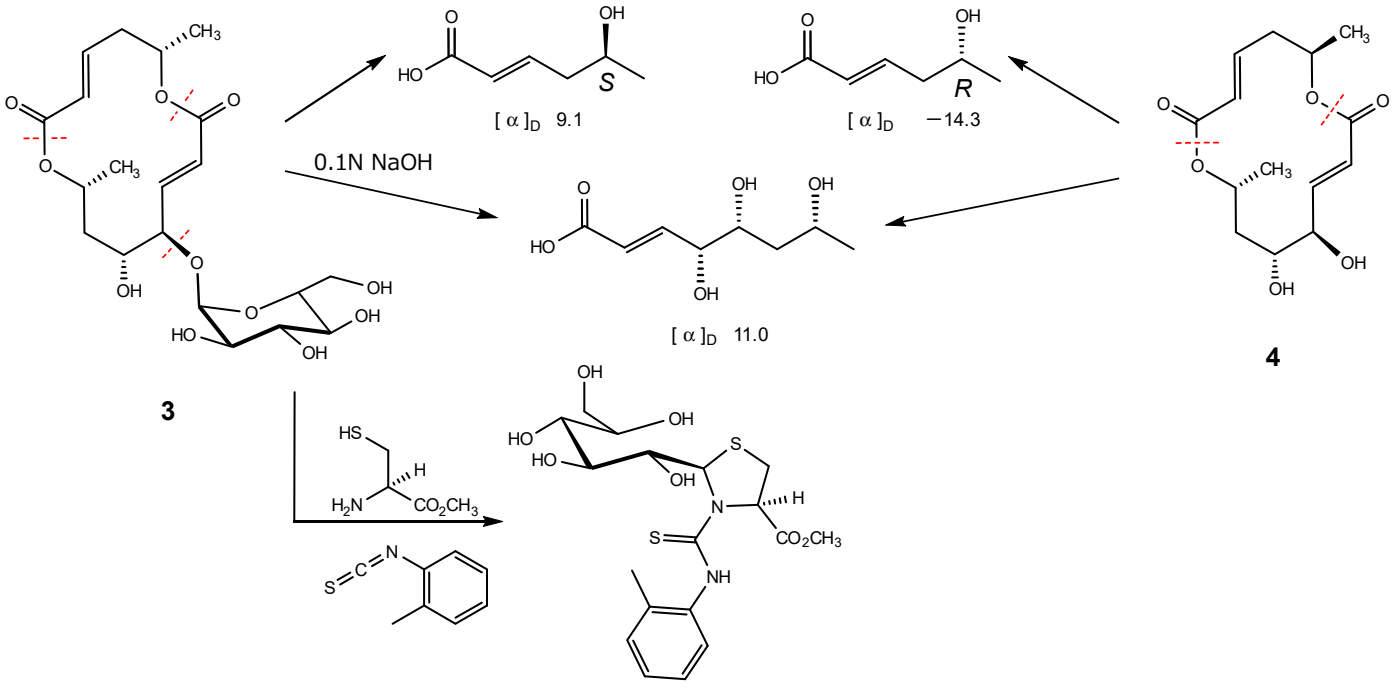

Scheme 2. The hydrolysis of **3** and **4**, and the derivatization of the sugar in **3**.

As a primary screen for the antitumor activity, the cancer cell growth inhibitory properties of halosmysins B (**2**) and C (**3**) isolated in this study were examined using murine P388 leukemia, human HL-60 leukemia, and murine L1210 leukemia cell lines. A previous study reported that **1** had potent cytotoxicity against these cell lines, whereas **4** did not inhibit cell growth [6]. As expected, **2**, having the same piperazinedione derivative, showed potent activity comparable to 5-fluorouracil against all these cells, particularly the HL-60 cell line. Compound **3**, colletodiol glycoside, did not inhibit cell growth (Table 2). The addition of various functional groups to the double bond between C-9 and C-10 provides information on the structure-activity relationship and the detailed mechanism of activity. Therefore, the search for 14-membered macrolide analogs from this fungal metabolite will continue.

Table 2. Cytotoxicity of metabolites **1**–**3** against cancer cell lines.

Compounds	P388	HL-60	L1210
	IC_{50} (μM) [a]	IC_{50} (μM) [a]	IC_{50} (μM) [a]
1	5.6 ± 1.6	3.2 ± 1.1	13.6 ± 2.2
2	10.7 ± 2.2	8.2 ± 1.8	20.5 ± 3.6
3	>300	61.6 ± 7.3	80.7 ± 7.7
5-fluorouracil [b]	5.2 ± 2.8	3.8 ± 2.1	6.4 ± 2.9

[a] DMSO was used as vehicle. [b] Positive control.

3. Materials and Methods

3.1. General Experimental Procedures

These are the same procedures as those in recent reports [6]. NMR spectra were recorded on an Agilent-NMR-vnmrs (Agilent Technologies, Santa Clara, CA, USA) 600 and 400 with tetramethylsilane (TMS) as an internal reference. FABMS was recorded using a JEOL JMS-7000 mass spectrometer (JEOL, Tokyo, Japan). IR spectra were recorded on an IRAffinity-1S (Shimadzu, Kyoto, Japan). Optical rotations were measured using a JASCO DIP-1000 digital polarimeter (Tokyo, Japan). Silica gel 60 (230–400 mesh, Nacalai Tesque, Inc., Kyoto, Japan) was used for column chromatography with medium pressure. ODS HPLC was run on a JASCO PU-1586 (Tokyo, Japan) equipped with a differential refractometer RI-1531 (Tokyo, Japan) and Cosmosil Packed Column 5C18-MSII (25 cm × 20 mm i.d., Nacalai Tesque, Inc., Kyoto, Japan). Analytical TLC was performed on precoated Merck aluminum sheets (DC-Alufolien Kieselgel 60 F254, 0.2 mm, Merck, Darmstadt, Germany) with the solvent system CH_2Cl_2–MeOH (19:1) (Nacalai Tesque, Inc., Kyoto, Japan), and compounds were viewed under a UV lamp (AS ONE Co., Ltd., Osaka, Japan) and sprayed with 10% H_2SO_4 (Nacalai Tesque, Inc., Kyoto, Japan) followed by heating.

3.2. Fungal Material

The fungus *Halosphaeriaceae* sp. was isolated from the surface of the marine alga *Sargassum thunbergii*. *Halosphaeriaceae* sp. collected at Osaka bay, Japan in July 2017. The fungal strain was identified based on the result of ITS rDNA nucleotide sequence analysis by Techno Suruga Laboratory Co., Ltd. (Shizuoka, Japan). The alga *Sargassum thunbergii* was wiped with EtOH and a cutting was applied to the surface of nutrient agar layered in a Petri dish. Serial transfers of one of the resulting colonies provided a pure strain of *Halosphaeriaceae* sp.

3.3. Culturing and Isolation of Metabolites

The fungus was cultured at 27 °C for four weeks in a medium (70 L) containing 1% glucose, 1% malt extract, and 0.05% peptone in artificial seawater adjusted to pH 7.5. Then, the culture filtrate was extracted thrice with AcOEt. The combined extracts were evaporated *in vacuo* to afford a mixture of crude metabolites (12.2 g). The EtOAc extract was chromatographed on a silica gel column with a CH_2Cl_2/MeOH gradient as the eluent to afford Fr. 1 (1% MeOH in CH_2Cl_2 eluate,188.5 mg) and Fr. 2 (5% MeOH in CH_2Cl_2

eluate, 24.7 mg). Fr. 1 was purified by ODS HPLC using MeOH/H_2O (90:10) as the eluent to afford **4** (9.7 mg) and Fr. 3 (8.8 mg). Fr. 3 was purified by ODS HPLC using MeOH/H_2O (80:20) as the eluent to afford **2** (0.8 mg) and **1** (5.7 mg). Fr. 2 was purified by ODS HPLC using MeOH/H_2O (60:40) as the eluent to afford **3** (5.5 mg). These compounds were supplemented by several cultures to use in the following reactions and assays.

Halosmysin B (**2**): pale yellow oil; $[\alpha]_D^{22}$ + 5.6 (*c* 0.06, $CHCl_3$); IR (neat) ν_{max}/cm^{-1}: 3378, 2925, 1712, 1665, 1601, 1512. HRFABMS *m*/*z* 615.2378 $[M + H]^+$ (calcd for $C_{31}H_{39}N_2O_9S$: 615.2376); NMR data, see Table 1 and Table S1.

Halosmysin C (**3**): pale yellow oil; $[\alpha]_D^{22}$ + 16.3 (*c* 0.041, EtOH); IR (neat) ν_{max}/cm^{-1}: 3420, 2925, 1706, 1652. HRFABMS *m*/*z* 469.1692 $[M + H]^+$ (calcd for $C_{20}H_{30}O_{11}Na$: 469.1680); NMR data, see Table 1 and Table S1.

3.4. Alkaline Hydrolysis of **2**

Using the same procedure of **1** [6], **2** (1.2 mg) and 0.1 N NaOH aq. (1 mL) were stirred at room temperature for 14 h, then acidified with conc. HCl and extracted with AcOEt. The organic layer was evaporated in vacuo, and the residue was purified by ODS HPLC using MeOH/H_2O (0.1% AcOH) (30:70) as the eluent to (–)-5-hydroxy-(2E)-hexenoic acid (0.4 mg) (r.t. 27.5 min).

(–)-5-hydroxy-(2E)-hexenoic acid: clear oil; $[\alpha]_D^{22}$ − 13.9 (c 0.06, EtOH); ^{1}H NMR (400 MHz, MeOH-d_4) δ ppm: 1.18 (3H, d), 2.31 (2H, dd), 3.85 (1H, sext), 5.82 (1H, d), 6.95 (1H, dt).

3.5. Alkaline Hydrolysis of **3**

Using the same procedure of **1** [6], **3** (2.2 mg) and 0.1 N NaOH aq. (1 mL) were stirred at room temperature for 4 h, then acidified with conc. HCl and extracted with AcOEt. The organic layer was evaporated in vacuo, and the residue was purified by ODS HPLC using MeOH/H_2O (0.1% AcOH) (30:70) as the eluent to (+)-4,5,7-trihydroxy-(2E)-octenoic acid (0.9 mg) (r.t. 14.5 min) and (+)-5-hydroxy-(2E)-hexenoic acid (0.3 mg) (r.t. 27.2 min).

(+)-4,5,7-trihydroxy-(2E)-octenoic acid; clear oil; $[\alpha]_D^{22}$ 11.0 (c 0.04, EtOH); ^{1}H NMR (400 MHz, MeOH-d_4) δ ppm: 1.20 (3H, d), 1.60 (2H, dd), 3.75 (1H, m), 3.96 (1H, dt), 4.18 (1H, dd), 6.05 (1H, d), 7.02 (1H, dd).

(+)-5-hydroxy-(2E)-hexenoic acid; clear oil; $[\alpha]_D^{22}$ 9.1 (c 0.11, EtOH).

3.6. Sugar Analysis of **3**

Glycoside **3** was analyzed with reference to the method described in Ref. [22]. **3** (4.8 mg) and 0.5 N HCl (1 mL) were stirred at 80 °C for 2 h. The reaction mixture was evaporated in vacuo, and the residue was dissolved in pyridine (1 mL) containing L-cysteine methyl ester hydrochloride (5.0 mg), and was heated at 60 °C for 1 h. *o*-torylisothiocyanate (5.0 mg) was added to the reaction mixture, and was heated at 60 °C for 1 h. The reaction mixture was directly analyzed by ODS HPLC using MeOH/H_2O (70:30). The peak at 17.7 min was coincident with derivative of D-glucose.

3.7. Assay for Cytotoxicity

Cytotoxic activities of **1**, **2** and **3** were examined by the same procedure to date [6], the 3-(4,5-dimethyl-2-thiazolyl)-2,5-diphenyl-2H-tetrazolium bromide (MTT) method. P388, HL-60, and L1210 cells were cultured in RPMI 1640 Medium (10% fetal calf serum) at 37 °C in 5% CO_2. The test materials were dissolved in dimethyl sulfoxide (DMSO) to give a concentration of 10 mM, and the solution was diluted with the Essential Medium to yield concentrations of 200, 20, and 2 μM, respectively. Each solution was combined with each cell suspension (1×10^5 cells/mL) in the medium, respectively. After incubating at 37 °C for 72 h in 5% CO_2, grown cells were labeled with 5 mg/mL MTT in phosphate-buffered saline (PBS), and the absorbance of formazan dissolved in 20% sodium dodecyl sulfate (SDS) in 0.1 N HCl was measured at 540 nm with a microplate reader (MTP-310, CORONA electric). Each absorbance value were expressed as a percentage relative to that of the control cell suspension that was prepared without the test substance using the same procedure as that

described above. All assays were performed three times, and semilogarithmic plots were constructed from the averaged data, and the effective dose of the substance required to inhibit cell growth by 50% (IC_{50}) was determined.

3.8. The Origin of the Cell Lines

The P388 cell line was obtained from Dr. Numata (death, Osaka Medical and Pharmaceutical University, Japan). The HL-60 cell line was obtained from Dr. Kawai (death, Fuso Pharmaceutical Industries, Ltd., Osaka, Japan). The L1210 cell line was from Dr. Endo (Kanazawa University, Japan).

4. Conclusions

In conclusion, we have isolated two new cytotoxic metabolites, halosmysins B and C, from the marine-alga-derived fungus *Halosphaeriaceae* sp., which had the same 14-membered macrodiolide skeleton as halosmysin A. We determined the absolute configuration of them using the chemical technique. **2** exhibited a potent cytotoxicity against the HL-60 cell line. In order to study the structure-activity relationship and the biosynthetic pathway, the search for 14-membered ring macrolide analogs from this fungal metabolite will be continued.

Supplementary Materials: The following supporting information can be downloaded at: https://www.mdpi.com/article/10.3390/md20040226/s1, Table S1: Spectral data including 2D NMR data for **2**, Table S2: Spectral data including 2D NMR data for **3**, Figure S1: 14-membered macrodiolides associated to halosmysins, Figure S2: ^{1}H NMR spectrum of **2** in $CDCl_3$, Figure S3: ^{13}C NMR spectrum of **2** in $CDCl_3$, Figure S4: ^{1}H-^{1}H COSY of **2**, Figure S5: NOESY of **2**, Figure S6: HMQC of **2**, Figure S7: HMBC of **2**, Figure S8: FABMS of **2**, Figure S9: IR spectrum of **2, Figure S10**: ^{1}H NMR spectrum of **3** in MeOH-d_4, Figure S11: ^{13}C NMR spectrum of **3** in MeOH-d_4, Figure S12: ^{1}H-^{1}H COSY of **3**, Figure S13: NOESY of **3**, Figure S14: HMQC of **3**, Figure S15: HMBC of **3**, Figure S16: FABMS of **3**, Figure S17: IR spectrum of **3**, Figure S18: HPLC chromatograms of halosmycins A, B, and C, Figure S19: ^{1}H NMR spectrum of 5-hydroxy-(2*E*)-hexenoic acid in MeOH-d_4, Figure S20: ^{1}H NMR spectrum of 4,5,7-trihydroxy-(2E)-octenoic acid in MeOH-d_4.

Author Contributions: Conceived and designed the experiments: T.Y., T.K. and T.H.; Performed the experiments: T.Y., K.Y.; Analyzed the data: T.Y.; and wrote the paper: T.Y. All authors have read and agreed to the published version of the manuscript.

Funding: This research received no external funding.

Institutional Review Board Statement: Not applicable.

Informed Consent Statement: Not applicable.

Conflicts of Interest: The authors declare that they have no conflict of interest.

References

1. Nicoletti, R.; Vinale, F. Bioactive Compounds from Marine-Derived *Aspergillus*, *Penicillium*, *Talaromyces* and *Trichoderma* Species. *Mar. Drugs* **2018**, *16*, 408. [CrossRef] [PubMed]
2. Imhoff, J.F. Natural Products from Marine Fungi—Still an Underrepresented Resource. *Mar. Drugs* **2016**, *14*, 19. [CrossRef] [PubMed]
3. Blunt, J.W.; Copp, B.R.; Keyzers, R.A.; Munro, M.H.G.; Prinsep, M.R. Marine natural products. *Nat. Prod. Rep.* **2017**, *34*, 235–294. [CrossRef]
4. Blunt, J.W.; Carroll, A.R.; Copp, B.R.; Davis, R.A.; Keyzers, R.A.; Prinsep, M.R. Marine natural 369 products. *Nat. Prod. Rep.* **2018**, *35*, 8–53. [CrossRef]
5. Yamada, T.; Tanaka, A.; Nehira, T.; Nishii, T.; Kikuchi, T. Altercrasins A–E, decalin derivatives, from a sea-urchin-derived *Alternaria* sp.: Isolation and structural analysis including stereochemistry. *Mar. Drugs* **2019**, *17*, 218. [CrossRef] [PubMed]
6. Yamada, T.; Kogure, H.; Kataoka, M.; Kikuchi, T.; Hirano, T. Halosmysin A, a novel 14-membered macrodiolide isolated from the marine-algae-derived fungus *Halosphaeriaceae* sp. *Mar. Drugs* **2020**, *18*, 320. [CrossRef] [PubMed]
7. MacMillan, J.; Simpson, T.J. Fungal Products. Part, V. The absolute stereochemistry of colletodiol and the structures of related metabolites of *Colletotrichum capsici*. *J. Chem. Soc. Perkin Trans 1* **1973**, 1487–1493. [CrossRef]

8. Ronald, R.C.; Gurusiddaiah, S. Grahamimycin A_1: A novel dilactone antibiotic from *Cytospora*. *Tetrahedron Lett.* **1980**, *21*, 681–684. [CrossRef]
9. Gurusiddaiah, S.; Ronald, R.C. Grahamimycins: Antibiotics from *Cytospora* sp. Ehrenb. W.F.P.L. 13A. *Antimicrob. Agents Chemother.* **1981**, *19*, 681–684. [CrossRef]
10. Hanson, K.; O'neill, J.A.; Simpson, T.J.; Willis, C.L. Bartanol and bartallol, novel macrodiolides from *Cytospora* sp. ATCC 20502. *J. Chem. Soc. Perkin Trans 1* **1994**, *17*, 2493–2497. [CrossRef]
11. Höller, U.; König, G.M.; Wright, A.D. A new tyrosine kinase inhibitor from a marine isolate of *Ulocladium botrytis* and new metabolites from the marine fungi *Asteromyces cruciatus* and *Varicosporina ramulosa*. *Eur. J. Org. Chem.* **1999**, *11*, 2949–2955. [CrossRef]
12. Grabley, S.; Hammann, P.; Thiericke, R.; Wink, J. Secondary metabolites by Chemical screening. 21 Clonostachydiol, a novel anthelmintic macrolide from the fungus *Clonostachys cylindrospora* (strain FH-A 6607). *J. Antibiot.* **1992**, *46*, 343–345. [CrossRef] [PubMed]
13. Lang, G.; Mitova, M.I.; Ellis, G.; van der Sar, S.; Phipps, R.K.; Blunt, J.W.; Cummings, N.J.; Cole, A.L.J.; Munro, M.H.G. Bioactivity profiling using HPLC/microtiter-plate analysis: Application to a New Zealand marine alga-derived fungus, *Gliocladium* sp. *J. Nat. Prod.* **2006**, *69*, 1007–1010. [CrossRef]
14. Ojima, K.; Yangchum, A.; Laksanacharoen, P.; Tasanathai, K.; Tanakitpipattana, D.; Tokuyama, H.; Isaka, M. Cordybislactone, a stereoisomer of the 14-membered bislactoneclonostachydiol, from the hopper pathogenic fungus *Cordyceps* sp. BCC 49294: Revision of the absolute configuration of clonostachydiol. *J. Antibiot.* **2018**, *71*, 351–358. [CrossRef]
15. Isaka, M.; Yangchum, A.; Auncharoen, P.; Srichomthong, K.; Srikitikulchai, P. Ring B aromatic norpimarane glucoside from a *Xylaria* sp. *J. Nat. Prod.* **2011**, *74*, 300–302. [CrossRef] [PubMed]
16. Han, J.; Su, Y.; Xu, Y.; Huo, X.; She, X. Asymmetric total synthesis and revision of the absolute configuration of 4-Keto-clonostachydiol. *J. Org. Chem.* **2009**, *74*, 3930–3932. [CrossRef] [PubMed]
17. Berg, A.; Notni, J.; Dorfelt, H.; Grafe, U. Acremonol and acremodiol, new fungal bislactones. *J. Antibiot.* **2002**, *55*, 660–662. [CrossRef]
18. Wang, T.T.; Wei, Y.J.; Ge, H.M.; Tan, R.X. Acaulide, an osteogenic macrodiolide from *Acaulium* sp. H-JQSF, an isopod-associated fungus. *Org. Lett.* **2018**, *20*, 1007–1010. [CrossRef]
19. Chu, M.; Mierzwa, R.; Truumees, I.; Gentile, F.; Patel, M.; Gullo, V.; Chan, T.-M.; Puar, M.S. Two novel diketopiperazines isolated from the fungus *Tolypocladium* sp. *Tetrahedron Lett.* **1993**, *34*, 7537–7540. [CrossRef]
20. Simpson, T.J.; Stevenson, G.I. Studies of polyketide chain-assembly processes: Origins of the hydrogen and oxygen atoms in colletodiol. *J. Chem. Soc. Chem. Commun.* **1985**, *24*, 1822–1824. [CrossRef]
21. Salvatore, M.M.; Nicoletti, R.; DellaGreca, M.; Andolfi, A. Occurrence and properties of thiosilvatins. *Mar. Drugs* **2019**, *17*, 664. [CrossRef] [PubMed]
22. Tanaka, T.; Nakashima, T.; Ueda, T.; Tomii, K.; Kouno, I. Facile discrimination od aldose enantiomers by reversed-phase HPLC. *Chem. Pharm. Bull.* **2007**, *55*, 899–901. [CrossRef] [PubMed]